ISBN: 978-3-95450-248-6 ISSN: 2673-5490 doi: 10.18429/JACoW-IPAC2025-WEPM080

IMPACT OF THE cSTART IMPEDANCE ON BEAM DYNAMICS

M. Schwarz*, A.-S. Müller, J. Schäfer, Karlsruhe Institute of Technology, Karlsruhe, Germany
S. Glukhov, TU Darmstadt, Darmstadt, Germany

Abstract

The combination of a compact storage ring and a laser-plasma accelerator (LPA) can serve as the basis for future compact light sources. One challenge is the large momentum spread (about 2%) of the electron beams delivered by the LPA. To overcome this challenge, a very large acceptance compact storage ring (VLA-cSR) was designed as part of the compact STorage ring for Accelerator Research and Technology (cSTART) project, which will be realized at the Karlsruhe Institute of Technology (KIT, Germany). Initially, the Ferninfrarot Linac- Und Test-Experiment (FLUTE), a versatile source of ultra-short bunches, will serve as an injector for the VLA-cSR to benchmark and emulate LPA-like beams. In a second stage, a laser-plasma accelerator will be used as an injector. The large-momentum spread bunches in non-equilibrium and with charges from 1 pC to 1000 pC and lengths from few fs to few ps pose challenges for the beam dynamics simulations. An understanding of the ultra-short bunch dynamics also requires an impedance model up to high frequencies. Here, we present first results on the impact of the machine impedance to the beam dynamics.

INTRODUCTION

Non-equilibrium effects often limit accelerator performance and parameter range. The cSTART project aims to understand, and ultimately control, non-equilibrium electron beams to enable new accelerator concepts and operation modes beyond the current state of the art. The heart of the project is the very-large acceptance compact storage ring (VLA-cSR), which is designed for the injection of LPA-generated electron beams and storage of 100 fs short electron bunches. To ensure that the bunch remains in non-equilibrium throughout the storage time of 100 ms, a low electron beam energy of 40 MeV to 90 MeV is chosen, resulting in damping times of several seconds. Normal conducting linacs and LPAs have repetition rates of only a few Hz, and by injecting these fs-short beams into a storage ring, the repetition rate is brought into the MHz regime. This makes LPAs attractive candidates for light sources [1], since sub-ps-short bunches emit intense coherent synchrotron radiation (CSR) in the THz regime. Hence, cSTART can pave the way towards powerful compact light sources with low power consumption.

Details on the cSTART project can be found in [2]. Updates on the vacuum system [3], the storage ring magnets [4], the LPA injection line [5], the FLUTE injection line [6] and its magnets [7], the diagnostic systems [8] as well as the alignment tolerances [9] are presented at this conference.

* markus.schwarz@kit.edu

Here, we focus on the impact of different impedance sources on the longitudinal beam dynamics. Any impedance leads to a wake potential, whose shape and strength depends on the characteristics of the impedance and the longitudinal bunch profile. The wake potential acts back on the bunch and changes the bunch profile, which again leads to a changing wake potential. We simulate this dynamics with the longitudinal tracking code BLonD [10], for details see [11].

LONGITUDINAL IMPEDANCE MODEL

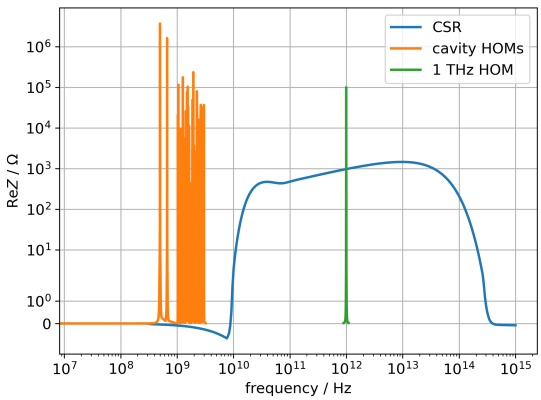

Figure 1: Different impedance sources at cSTART: broad-band CSR (blue), narrow-band 500 MHz cavity HOMs (orange), and a fictitious source at 1 THz (green).

Figure 1 shows different contributions of the cSTART impedance model. The higher order modes (HOM) of the 500 MHz cavity are known up to 3 GHz [12], with the main resonance at $f_r = 498.63$ MHz having a shunt impedance $R_r = 3.7\,\mathrm{M}\Omega$ and quality factor $Q_r = 2.98 \times 10^4$.

The effect of coherent synchrotron radiation can also be modeled by an impedance [13]. Here, we use the CSR impedance $Z_{\mathrm{CSR,pp}}$ with shielding due to parallel-plates [14], which leads to a suppression of frequencies below the cut-off frequency of 25 GHz. While the overall strength of the CSR impedance is less than the cavity HOMs, its broad-band nature means that it has significant impact on sub-ps short bunches.

Presently, the impedance of other components, such as bellows, vacuum pump port, or the injection kicker, is unknown. It is also difficult to compute their impedances up to frequencies in the THz regime. Usually, this is not needed for single-pass machines or storage ring with bunch lengths well above tens of ps. To investigate what, if any, effects these high-frequency impedance sources have on the beam, we introduce a fictitious narrow-band resonator at 1 THz.

ISBN: 978-3-95450-248-6 ISSN: 2673-5490 doi: 10.18429/JACoW-IPAC2025-WEPM080

LOSS FACTOR

The characterization of a non-equilibrium bunch is a non-straightforward topic. Bunch length is not a good quantity for non-equilibrium bunches with micro-bunches because the RMS bunch length gives strong weight to halo particles, while the FWHM is ill defined when the bunch profile contains spikes due to micro-bunches.

Instead, we use quantities derived from the *loss factor*. The loss factor κ depends on the impedance Z and longitudinal bunch profile [13]:

$$\kappa = 2\int_0^\infty \Re Z(f)\,|\Lambda(f)|^2 \mathrm{d}f, \tag{1}$$

where Λ denotes the Fourier transform of the longitudinal bunch profile (normalized to one). It has dimension energy/charge^2. Multiplying by the square of the bunch charge Q_b gives the total energy that is lost by the bunch. This energy represents either ohmic losses in a structure (for a geometric impedance) or the coherently emitted radiation (for CSR impedance). At cSTART we want to minimize the former and maximize the latter. In general, a shorter bunch has a larger spectral range, which leads to a larger loss factor and more emitted CSR, since the CSR impedance is broad-band. However, it can also be beneficial to have a dense bunch core surrounded by a halo to increase the overall emitted CSR [15].

Another useful derived quantity is the average lost energy per particle

$$\bar{U}_{\mathrm{lost}} = Q_b^2\,\kappa/N \tag{2}$$

where N denotes the number of particles in the bunch. The center-of-charge position is directly proportional to $\bar{U}_{\mathrm{lost}}$ [16]. Hence, $\bar{U}_{\mathrm{lost}}$ can be measured by recording the bunch profile or transverse bunch position in a dispersive section.

The loss factor can be computed analytically for a Gaussian bunch with duration σ and some impedances. For a resonator impedance it is given by [13]

$$\kappa_{\mathrm{res}} = \frac{R_r\alpha}{\omega_{\mathrm{eff}}}\Re\left[\omega_+ w(\sigma\omega_+)\right] \simeq \begin{cases} R_r\,\alpha & \sigma\omega_+ \ll 1 \\ \frac{R_s\,\alpha^2}{\sqrt{\pi}\omega_r^4\sigma^3} & \sigma\omega_+ \gg 1 \end{cases} \tag{3}$$

with $\alpha = \omega_r/2Q_r$, $\omega_+ = \sqrt{\omega_r^2 - \alpha^2} + \mathrm{i}\alpha$. The approximate expressions are valid for short and long bunches, respectively. For the unshielded free-space CSR impedance $Z_{\mathrm{CSR,fs}}$, the loss factor for a Gaussian bunch is given by

$$\kappa_{\mathrm{CSR,fs}} = \frac{Z_0}{4\pi}\frac{\omega_c\gamma}{4\Sigma^3}\left[\sqrt{\pi}\exp\left(\frac{1}{8\Sigma^2}\right)K_{5/6}\left(\frac{1}{8\Sigma^2}\right) - 2\pi\Sigma\right], \tag{4}$$

where $\Sigma = \sigma\,\omega_c$, and ω_c and γ denote the critical frequency and Lorentz factor, respectively. For the shielded parallel-plates impedance, the loss factor can be computed numerically from Eq. (1).

The results for a 1 pC Gaussian bunch at 40 MeV and different bunch lengths are shown in Table 1. The CSR impedance was divided by the number of dipoles (eight), to obtain the emitted radiation at one light port. Generally, CSR dominates the energy loss for all bunch lengths. Due to the broad-band nature of the CSR impedance, shorter bunches have a larger overlap in Eq. (1) and emit more CSR. The cut-off frequency due to the shielding is at 25 GHz for the cSTART dipoles and thus affects only long bunches. Consequently, we see that the CSR emission is reduced by about four times only for the long 10 ps bunch. However, the cavity HOMs are known only up to 3 GHz and even the 10 ps is practically point-like at these frequencies. As a result, the ohmic losses due to the cavity HOMs are constant for all bunch lengths. Contrary, the fictitious 1 THz HOM yields negligible losses for bunches that are longer than 1 ps, and thus have a vanishingly small spectrum at that frequency. Keep in mind that even if the loss factor of a given impedance may be tiny, its impact on the beam dynamics can still be significant [17].

Table 1: Average Energy Loss for Different Impedance Sources

	10 ps	**1 ps**	**0.1 ps**	**0.01 ps**
$\bar{U}_{\mathrm{CSR,pp}}$	1.5 eV	122 eV	2.4 keV	37 keV
$\bar{U}_{\mathrm{CSR,fs}}$	5.7 eV	122 eV	2.4 keV	37 keV
$\bar{U}_{\mathrm{HOM}}$	0.6 eV	0.6 eV	0.6 eV	0.6 eV
$\bar{U}_{\mathrm{1THz}}$	4 neV	4 µeV	21 eV	31 eV

SIMULATION RESULTS

As initial conditions, we use the simulation of a 1 pC bunch at 41.5 MeV that was tracked through the FLUTE injection line [18]. It has an RMS energy spread of 2.6 % with RMS bunch length $\sigma_{\mathrm{RMS}} = 17$ fs and 1σ-equivalent FWHM bunch length $\sigma_{\mathrm{FWHM}} = 7.9$ fs. As discussed above, the difference is due to a dense core with a tail. We repeat each simulation with six different seeds for the starting distribution.

We study three scenarios: first, we simulate the bunch only subject to the influence of the parallel-plates CSR impedance. Second, we *add* to this the impdedances from the cavity HOMs. Finally, we simulate with the CSR, HOM, and the fictitious 1 THz impdedance.

Figure 2 shows the average energy loss due to CSR per dipole $\bar{U}_{\mathrm{CSR,pp}}$ for these three scenarios for the first 200 turns (30 µs). The initial energy loss of 37 keV is off the graph. After passing through the first dipole, the bunch lengthens and the CSR quickly ceases. However, the bunch recovers its compact bunch shape after half a synchrotron period (22 turns) and the CSR emission peaks again. Due to filamentation, the bunch gradually forms a dense core surrounded by a halo and the intensity of the CSR emission decreases with each half synchrotron period. The three cases are practically indistinguishable from each other since the CSR impedance creates the dominant wake potential, see last column of Table 1.

However, the three cases lead to a different bunch evolution over the whole 7×10^5 turns (100 ms). Figure 3 shows

ISBN: 978-3-95450-248-6 ISSN: 2673-5490 doi: 10.18429/JACoW-IPAC2025-WEPM080

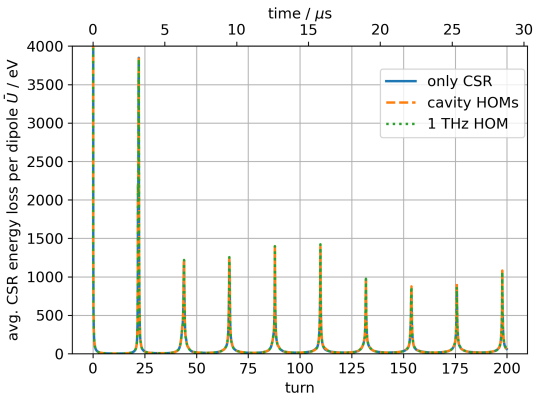

Figure 2: Average energy loss due to CSR per dipole for the three impedance scenarios for the *first* 200 turns after injection.

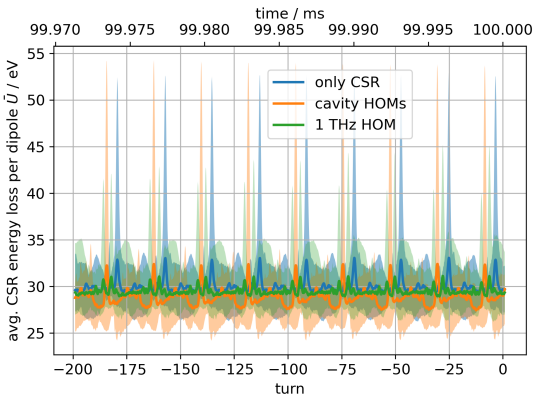

Figure 3: Average energy loss due to CSR per dipole for the three impedance scenarios the *last* 200 turns before extraction.

CSR energy loss for the *last* 200 turns before extraction. The solid curves depict the mean $\bar{U}_{\mathrm{CSR,pp}}$ of all six seeds, whereas the shaded area cover the minimum and maximum values. We observe a periodic increase in CSR emission every half synchrotron period but at much reduced intensity compared to the initial turns. These peaks are caused by one or more micro-bunches that orbit a central core. One example is shown in Fig. 4. When the micro-bunch is "above" or "below" the core, the resulting bunch profile, which is the longitudinal projection of the phase space density, has a single large peak and the CSR increases. The number and charge of the micro-bunches are similar in all three impedance scenarios, and depend on the subtle differences of the initial conditions enhanced by the non-linear dynamics. Meanwhile, neither the low-frequency cavity HOMs nor the fictitious 1 THz impedance appear to have a significant influence on the beam evolution.

SUMMARY AND OUTLOOK

A key part of the cSTART project is the construction of a very-large momentum acceptance compact storage ring to capture LPA-generated electron beams and store 100 fs short bunches. The low beam energy leads to long damping times and the bunch remains in non-equilibrium throughout the 100 ms of storage time. In this contribution, we simulated the impact of different geometric impedance sources on the longitudinal beam dynamics with BLonD. One source are the HOMs of the 500 MHz cavity, which are known up to 3 GHz. However, the fs short bunches have significant spectral content also at frequencies of 1 THz and beyond. We introduce a fictitious narrow-band resonator at 1 THz to study the influence of potential sources at these high frequencies, since current state-of-the-art impedance simulation tools are not able to compute an impedance up to these frequencies.

We use the loss factor to quantify the impact of an impedance. The loss factor from the CSR impedance is the dominant contribution for all bunch lengths. Hence, the initial dynamics over the first few synchrotron periods is practically unaffected by the presence of any other impedance source. Also the dynamics after 100 ms is nearly identical. The formation of micro-bunches is present in all cases, and the exact details on their number and intensity depend more on the subtle differences in their initial conditions, which gets enhanced by the non-linear dynamics. Thus, their formation is linked to the dynamics of the first turn, but their existence throughout the total storage time is a consequence of the bunch not reaching its equilibrium.

As next steps, we plan to investigate the effects on space-charge, since it is likely non-negligible at the low energies of only up to 90 MeV. Intra-bunch scattering is also a very important aspect of the beam dynamics which needs to be included. These effects require to go beyond the longitudinal plane and to consider the full 6D phase space dynamics.

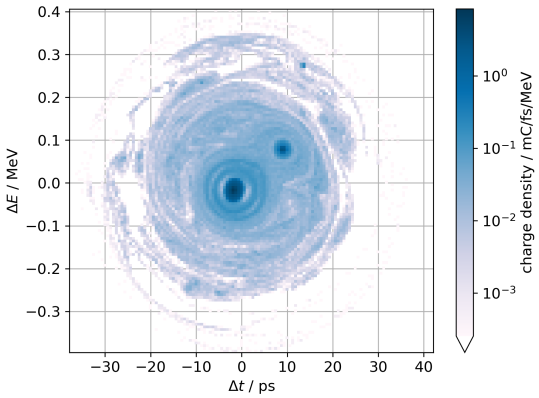

Figure 4: Phase space density after 100 ms for the scenario including the fictitious source at 1 THz.

REFERENCES

[1] S. Hillenbrand, R. Assmann, A.-S. Müller, O. Jansen, V. Judin, and A. Pukhov, "Study of laser wakefield accelerators as injectors for synchrotron light sources", *Nucl. Instrum. Methods Phys. Res., Sect. A*, vol. 740, pp. 153–157, 2014. doi:10.1016/j.nima.2013.10.081

ISBN: 978-3-95450-248-6 ISSN: 2673-5490 doi: 10.18429/JACoW-IPAC2025-WEPM080

[2] M. Schwarz *et al.*, "Recent Developments of the cSTART Project", in *Proc. FLS'23*, Luzern, Switzerland, pp. 155–158, 2024. doi:10.18429/JACoW-FLS2023-TU4P34

[3] B. Krasch, C. Widmann, M. Fuchs, M. Nasse, and R. Ruprecht, "Conceptual design of the vacuum system of cSTART", presented at IPAC'25, Taipei, Taiwan, Jun. 2025, paper THPB001, this conference.

[4] A. Bernhard *et al.*, "Magnetic design of the cSTART magnets", presented at IPAC'25, Taipei, Taiwan, Jun. 2025, paper WEPB026, this conference.

[5] A. Papash *et al.*, "Beamline to inject laser plasma accelerated electrons to a quasi-isochronous compact storage ring", presented at IPAC'25, Taipei, Taiwan, Jun. 2025, paper TUPS003, this conference.

[6] J. Schaefer *et al.*, "Simulation-based optimization of the injection of ultrashort non-Gaussian electron beams into a storage ring", presented at IPAC'25, Taipei, Taiwan, Jun. 2025, paper WEPM031, this conference.

[7] A. Bernhard, J. Schaefer, B. Haerer, S. Fatehi, and A. Ahl, "Compact quadrupole-sextupole magnet units for the FLUTE-cSTART injection line", presented at IPAC'25, Taipei, Taiwan, Jun. 2025, paper WEPB027, this conference.

[8] D. E. Khechen *et al.*, "Characterisation of the foreseen turn-by-turn beam position instrumentation for the cSTART storage ring", presented at IPAC'25, Taipei, Taiwan, Jun. 2025, paper THPS094, this conference.

[9] P. Schreiber *et al.*, "Alignment tolerance studies for the cSTART storage ring", presented at IPAC'25, Taipei, Taiwan, Jun. 2025, paper WEPM038, this conference.

[10] H. Timko *et al.*, "Beam longitudinal dynamics simulation studies", *Phys. Rev. Accel. Beams*, vol. 26, no. 11, p. 114 602, 2023. doi:10.1103/PhysRevAccelBeams.26.114602

[11] M. Schwarz, S. T. Braner, B. Härer, A.-S. Müller, and J. Schäfer, "Longitudinal beam dynamics for different initial distributions at cSTART", in *Proc. IPAC'23*, Venice, Italy, pp. 3518–3521, 2023. doi:10.18429/JACoW-IPAC2023-WEPL167

[12] G. Blokesch and K. Dunkel, "cSTART RF system technical design report", Research Instruments, Tech. Rep. TR-6415, 2024.

[13] B. W. Zotter and S. A. Kheifets, *Impedances and Wakes in High-Energy Particle Accelerators*. World Scientific, 1998.

[14] J. Murphy, S. Krinsky, and R. Gluckstern, "Longitudinal wake field for an electron moving on a circular orbit", *Part. Accel.*, vol. 57, pp. 9–64, 1997.

[15] C. Xu, E. Bründermann, A.-S. Müller, A. S. Garcia, M. Schwarz, and J. Schäfer, "Optimization Studies of Simulated THz Radiation at FLUTE", in *Proc. IPAC'22*, Bangkok, Thailand, pp. 2292–2295, 2022. doi:10.18429/JACoW-IPAC2022-WEPOMS023

[16] M. Schwarz, A. Farricker, I. Karpov, and A. Lasheen, "Synchronous phase shift measurements for evaluation of the longtitudinal impedance model at the CERN SPS", in *Proc. ICFA mini-Workshop on Mitigation of Coherent Beam Instabilities in Particle Accelerators*, Zermatt, Switzerland, pp. 318–322, 2019. doi:10.23732/CYRCP-2020-009

[17] S. Maier, M. Brosi, A. Mochihashi, M. J. Nasse, M. Schwarz, and A.-S. Müller, "Simulation of the impact of an additional corrugated structure impedance on the bursting dynamics in an electron storage ring", *Phys. Rev. Accel. Beams*, vol. 27, no. 11, p. 112 803, 2024. doi:10.1103/PhysRevAccelBeams.27.112803

[18] J. Schäfer, "Lattice design of a transfer line for ultra-short bunches from flute to cstart", M.S. thesis, Karlsruhe Institute of Technologie, Germany, 2019, 81 pp. doi:10.5445/IR/1000105061